

Statistical estimation of link availability and its impact on routing in wireless ad-hoc networks

A. Bruce McDonald^{1,*†} and Taieb F. Znati²

¹*Department of Electrical and Computer Engineering, Northeastern University, Boston, MA 02115, U.S.A.*

²*Computer Science Department, University of Pittsburgh, Pittsburgh, PA 15260, U.S.A.*

Summary

In this paper, an analytical framework is developed and validated via simulation for statistical estimation of the evolution of the separation between a pair of mobile nodes in an ad-hoc network. Simulation results demonstrate that path selection based on minimization of the product of the link statistic significantly outperforms minimum-hop and fixed threshold-based ‘*path-stability*’ schemes. A hierarchical mobility model integrating the dynamic effects of velocity, group movement and geographic scope is used to generalize the results. Another significant result is the performance enhancements hold in large networks irregardless of the assumptions used for statistical estimation. The effect of merging many independent groups appears to restore independent mobility. Finally, results show that at the highest mobility levels, 90% of the longest surviving paths fail within 60 s. None of the strategies approach this optimal value. This important result suggests that optimal predictive mechanisms alone are insufficient to ensure scalable routing in ad-hoc networks. Copyright © 2003 John Wiley & Sons, Ltd.

KEY WORDS: [Q1](#)wireless ad hoc networks

Q1

1. Introduction

This paper examines the problem of finding *survivable* links for routing in wireless ad-hoc networks. Specifically, an analytical framework is developed for statistically predicting link availability subject to random mobility based on different initial conditions. We hypothesize the following: (1) prediction of link survival enables more efficient route selection by reducing re-routing frequency after link failures; (2) in large networks, aggregate mobility exhibits random-

ness despite significant group mobility, and hence, provides an effective approximation for application in uniformly distributed communications scenarios; and (3) path selection based upon a simple product-form aggregation of the quantitative metric will outperform fixed threshold based ‘*path-stability*’ schemes [1,2] proposed in the past. The deterioration or failure of a wireless data-link carrying traffic has the following undesirable effects: First, it may lead to the loss or corruption of data. As such, higher-layer protocols generally timeout and retransmit. Without wireless

*Correspondence to: A. Bruce McDonald, Department of Electrical and Computer Engineering, Northeastern University, Boston, MA 02115, U.S.A.

†E-mail: mcdonald@ece.neu.edu

Contract/grant sponsor: National Science Foundation (NSF) (by CISE/ANIR); contract/grant number: 0073972.

Contract/grant sponsor: Hewlett Packard (HP); contract/grant number: 35177.

Contract/grant sponsor: Center for Clinical Neurophysiology, Department of Neurosurgery, University of Pittsburgh Medical Center (UPMC).

enhancements, TCP engages *slow-start* mechanisms, thus limiting achievable throughput. Furthermore, there may be a substantial delay in re-establishing the interrupted communications paths. Finally, if a failed link carries a large number of end-to-end flows, the routing overhead required to repair the individual paths may be substantial enough to exacerbate the congestion effects already caused by the service disruption. This illustrates an inherent shortcoming typical of *on-demand* ad-hoc routing protocols that rely on virtual circuit ‘like’ mechanisms for path control. Routing over links that have the longest survival times can minimize these negative effects.

The purpose of this paper is to address this problem by considering the question of link availability—how long will two nodes remain in close enough proximity for a link between them to remain active? More precisely, with what probability will two nodes remain within a given distance threshold of one another over time? The analytical framework expands upon the work presented in Reference [3] which was the mechanism for adapting cluster size and configuration to localized-network dynamics. In this paper, the results are further generalized and validated via simulation; moreover, the metric is applied directly to route selection and compared to alternative schemes; the performance metric is the expected path survival time, which is invariant to the choice of routing algorithm. It is an indicator of the time between path restoration activity and, hence, the rate at which traffic flows are interrupted.

The results demonstrate statistical and substantive performance gains over the fixed threshold approach and shortest-path routing. Several important contributions are reported in this paper: without loss of generality, we present compelling evidence that the link stability prediction is a critical element of the future success of ad-hoc network technology. However, despite substantial performance gains, our metric is unable to capture the most rapidly changing network dynamics. Consequently, we claim that real-time measurement based localization and trajectory prediction mechanisms are needed which provide statistical confidence bounds on their predictions. Moreover, we show that under highly dynamic conditions, optimal path survival times are very short—90% of longest lived paths fail within 60 s. This is a very important result as it suggests that prediction alone is insufficient—scalable solutions to routing in ad-hoc networks must combine predictive mechanisms with other strategies, for example, adaptive clustering, multiple-level dynamic hierarchies

and dispersity based multi-path routing. The remainder of this paper is organized as follows: for completeness, Section 2 presents the random walk-based mobility model first proposed in Reference [3]. Section 3 presents expressions for link availability including on new model. In Section 4, the analytical results are validated via simulation. The metric is put to the test in Section 5 where the performance is measured and compared to other routing strategies. Finally, conclusions are presented in Section 6.

2. Ad-Hoc Mobility Model

According to the model proposed in Reference [3], presented here for completeness, each node’s movement consists of a sequence of random length intervals called *mobility epochs* during which time it moves in a constant direction at a constant speed. The speed and direction vary randomly from epoch to epoch. V_n^i and θ_n^i , are respectively, the speed and direction of node n during epoch i . Consequently, during epoch i of duration T_n^i , node n moves a distance of $V_n^i T_n^i$ in a straight line at an angle of θ_n^i . The number of epochs during an interval of length t is the discrete random process $\mathcal{N}_n(t)$. Figure 1(a) illustrates the movement of node n over six mobility epochs, each of which is characterized by its direction, θ_n^i , and distance, $V_n^i T_n^i$.

The *mobility profile* of a given node n is completely specified according to the following three parameters: λ_n , μ_n and σ_n^2 . The following list defines these parameters for node n , and describes the assumptions made in developing this model:

- The epoch lengths are IID exponentially distributed with mean $1/\lambda_n$ (the exponential distribution assumption is relaxed in Corollary 2.2);
- The speed during each epoch is an IID distributed random variable (e.g. IID uniform) with mean μ_n and variance σ_n^2 , and remains constant only for the duration of the epoch;
- The direction of the mobile during each epoch is IID uniformly distributed over $(0, 2\pi)$, and remains constant only for the duration of the epoch;
- Speed, direction and epoch length are uncorrelated;
- Mobility is uncorrelated among the nodes of a network and links fail independently.

The distribution of the number of mobility epochs is assumed to be stationary and large. Furthermore, it is assumed that the distributions of each node’s

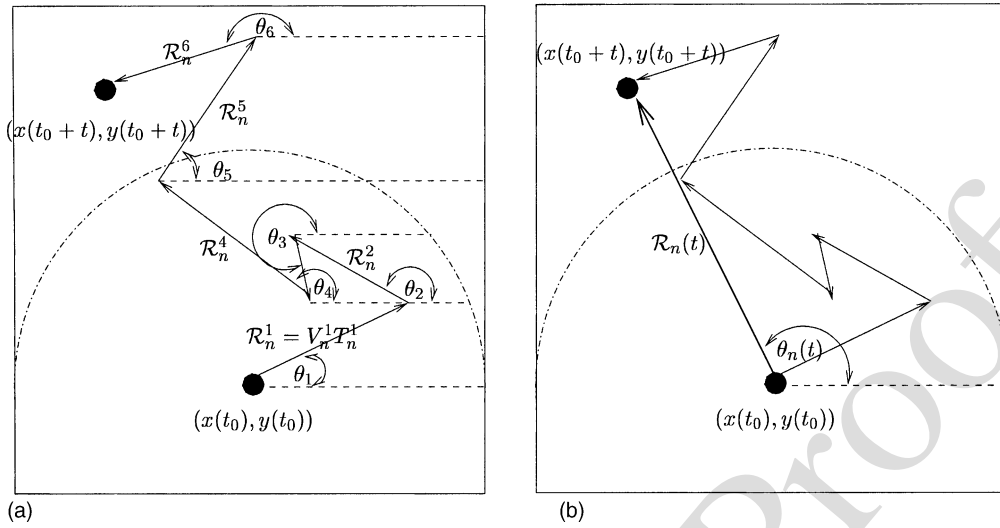


Fig. 1. Ad-hoc mobility model node movement: (a) epoch mobility vectors; (b) random mobility vector (t_0, t) .

velocity are stationary. Since the epoch lengths are IID exponentially distributed, $\mathcal{N}_n(t)$ is a Poisson process with rate λ_n . Hence, the expected number of epochs experienced by node n during the interval $(0, t)$, while a link is active, is $\lambda_n t \gg 1$. Equivalently, it is assumed that while each link is active, there are a large number of changes in speed and direction that take random values according to IID random variables.

In order to characterize the availability of a link between two nodes over a period of time (t_0, t) , the distribution of the mobility of one node with respect to the other must be determined. To characterize this distribution, it is first necessary to derive the mobility distribution of a single node in isolation. The single node distribution is extended to derive the joint mobility distribution which accounts for the mobility of one node with respect to the other. Using this joint mobility distribution, the link availability distribution is derived.

2.1. Single Node Mobility

Two random vectors are central to the development of the single node mobility model. These vectors characterize the direction and distance moved by a mobile node during a single epoch and over an interval of length t respectively.

Definition 2.1. $\vec{\mathcal{R}}_n^i$ is the epoch random mobility vector for node n . This vector represents the direction and distance moved by node n during mobility epoch i . Its magnitude, $\mathcal{R}_n^i = |\vec{\mathcal{R}}_n^i| = V_n^i T_n^i$, is the distance cov-

ered by node n during epoch i , and its phase, θ_n^i , is the direction of node n during epoch i .

Definition 2.2. $\vec{\mathcal{R}}_n(t)$ is the random mobility vector for node n . Its magnitude, $\mathcal{R}_n(t)$, is equal to the distance from $(x(t_0), y(t_0))$ to $(x(t_0 + t), y(t_0 + t))$, where $(x(\tau), y(\tau))$ is the position of the node at time τ . Its phase angle, $\theta_n(t)$, is the angle of the line joining the node's initial position, $(x(t_0), y(t_0))$, to its position at time t , $(x(t_0 + t), y(t_0 + t))$. The random mobility vector can be expressed as a random sum of the epoch random mobility vectors: $\vec{\mathcal{R}}_n(t) = \sum_{i=1}^{\mathcal{N}_n(t)} \vec{\mathcal{R}}_n^i$.

Figure 1(a) shows the movement of node n over an interval of length t , as it moves from position $(x(t_0), y(t_0))$ to position $(x(t_0 + t), y(t_0 + t))$. For each epoch, the figure shows the epoch vector $\vec{\mathcal{R}}_n^i$ with magnitude $V_n^i T_n^i$ and direction θ_n^i of the node during the epoch. The resulting random mobility vector $\vec{\mathcal{R}}_n(t)$ is shown in Figure 1(b); it can be seen that it is the vector sum of the individual epoch vectors. The following lemma characterizes the magnitude and phase distributions of $\vec{\mathcal{R}}_n(t)$:

Lemma 2.1. Consider a mobile node, n , which is initially located at position $(x(t_0), y(t_0))$ at time t_0 and moves according to a random ad-hoc mobility profile, $\langle \lambda_n, \mu_n, \sigma_n^2 \rangle$. Let $\vec{\mathcal{R}}_n(t)$ be the resulting random mobility vector. The phase angle, $\theta_n(t)$, of $\vec{\mathcal{R}}_n(t)$ represents the aggregate direction of the mobile node and is uniformly distributed over $(0, 2\pi)$; the magnitude, $\mathcal{R}_n(t)$, of $\vec{\mathcal{R}}_n(t)$ represents the aggregate distance moved by the node and is approximately Raleigh distributed with parameter $\alpha_n = (2t/\lambda_n)(\sigma_n^2 + \mu_n^2)$:

$$Pr(\theta_n(t) \leq \phi) = \frac{1}{2\pi} \phi \quad 0 \leq \phi \leq 2\pi$$

$$Pr(\mathcal{R}_n(t) \leq r) \approx 1 - \exp\left(\frac{-r^2}{\alpha_n}\right) \quad 0 \leq r \leq \infty$$

Complete derivation of Lemma 2.1 appears in Reference [4].

Corollary 2.1. *The results of Lemma 2.1 hold even if the distributions of the speed V_n^i , during each mobility epoch are not identically distributed, so long as the total distance covered is not dominated by the distance covered in any single epoch. The parameter of the Raleigh distribution in this case is: $\alpha_n = (\lambda_n t) * E[(\mathcal{R}_n^i)^2]$, where $E[(\mathcal{R}_n^i)^2] = E[(V_n^i T_n^i)^2]$ is the second moment of the distribution of the distance covered by the mobile during a single epoch.*

The conditions required to satisfy the CLT for the distributions of $X_n(t)$ and $Y_n(t)$ require that the number of terms in the summations be large, ($\lambda_n t \gg 1$), and that $E[(V_n^i T_n^i)^2] \ll \sum_{i=1}^{\mathcal{N}_n(t)} E[(V_n^i T_n^i)^2]$ for all i . These conditions will be violated if any term, $V_n^i T_n^i$, predominates. Corollary 2.1 follows directly. The significance of Corollary 2.1 is that the fundamental result holds when the distribution of speed is not fixed. Thus models that alternate between periods of movement and rest, or city and highway driving, for example, are covered by this model. Corollary 2.2 generalizes the distribution of the epoch lengths and gives the conditions under which the results hold for exponential epoch lengths.

Corollary 2.2. *Let the discrete random process $\mathcal{N}(t)$ count the number of mobility epochs during an interval of length, t , for a given node. The results of Lemma 2.1 hold for arbitrary distributions of epoch length, so long as $\sqrt{(E[(\mathcal{N}(t))^2]/E[\mathcal{N}(t)]^2 - 1)} \rightarrow 0$.*

Let $P_{\mathcal{N}(t)}$ be the distribution of $\mathcal{N}(t)$, and $X^\nu = \sum_{i=1}^{\nu} X^i$, with probability density function (pdf) $f_X^\nu(x)$, be the summation of the X components for an arbitrary fixed value of $\mathcal{N}(t) = \nu$. The pdf of the summation of the X components over an interval of length t , $X(t)$, is given by the following expression:

$$f_{X(t)}(x) = \sum_{\nu=0}^{\infty} P_{\mathcal{N}(t)} f_X^\nu(x) \quad (1)$$

The problem is to determine the conditions on $P_{\mathcal{N}(t)}$, such that $f_{X(t)}(x)$ is approximately Normally distributed, thereby satisfying Lemma 2.1. For large enough values of N , $f_X^\nu(x)$ will be approximately Normal for

all $\nu \geq N$. Consequently, it is possible to replace the general pdf, $f_X^\nu(x)$, in Equation (1) with a Normal pdf if the lower limit of the summation is changed from $\nu = 0$ to $\nu = N$. The condition in the corollary can be derived by first assuming that $f_{X(t)}(x)$, based on these modified limits, can be replaced by a Normal pdf. Making this replacement in Equation (1), expanding the exponentials and comparing them term-by-term shows the conditions for which the equation holds. An approximate solution is attained by assuming that for a given t , $P_{\mathcal{N}(t)}$ takes on significant values only for a bounded range of values for $\mathcal{N}(t)$.[‡] Based on this assumption, it can be shown that if $\sqrt{(E[(\mathcal{N}(t))^2]/E[\mathcal{N}(t)]^2 - 1)} \rightarrow 0$, the left-hand side of Equation (1) is approximately Normal [5]. The proof can be completed by observing that the same results also hold for the summation of the Y components. The corollary shows that for exponentially distributed epoch lengths $\lambda t \gg 1$ for the results to hold.

The results of this subsection show that if a mobile node moves in a random uniform direction during each mobility epoch, the randomness is preserved over several direction and speed changes. Along with the distribution of the aggregate distance, this allows for the characterization of the joint mobility of two mobile nodes in the next subsection by considering the *relative* movement of one node with respect to the other. The corollaries show that the model can be adapted to a number of different mobility scenarios. For example, it can model nodes in constant motion, or it can model mobility involving random *dwell-times*. Both node speed and epoch duration are easily generalized—speed can follow *any* distribution and epoch length can come from any distribution that meets the conditions of Corollary 2.2.

2.2. Joint Node Mobility

The characterization of mobility metrics for cellular networks relies on the analysis of the movement of a single node with respect to a fixed point of reference [6–9]. However, the analysis of ad-hoc mobility must consider the joint movement of a pair of adjacent mobile nodes. Based on the independence assumption, it is possible to consider the joint movement of two nodes by fixing the frame of reference of one node with respect to the other and considering relative

[‡]An exact solution is shown in Reference [5] to hold only for the trivial case where $\mathcal{N}(t)$ is deterministic.

movement. Thus, effectively transforming the ad-hoc mobility problem into the cellular problem. This transformation is accomplished by logically treating one of the nodes as if it were the *base station* of a cell, keeping it at a fixed position. For each movement of this node, the other node is translated an equal distance in the opposite direction. The result is the *equivalent random mobility vector* which is characterized by the following definition and lemmas:

Definition 2.3. $\vec{\mathcal{R}}_{m,n}(t)$ is the equivalent random mobility vector of node m with respect to node n . It is defined by fixing m 's frame of reference to n 's position, and moving m relative to that point.

Lemma 2.2. Let two mobile nodes, m and n , move according to random ad-hoc mobility profiles, $\langle \lambda_m, \mu_m, \sigma_m^2 \rangle$ and $\langle \lambda_n, \mu_n, \sigma_n^2 \rangle$, respectively. By Lemma 2.1, the random mobility vectors for each node are $\vec{\mathcal{R}}_m(t)$ and $\vec{\mathcal{R}}_n(t)$ with uniformly distributed direction and Raleigh distributed magnitude. Let α_m and α_n be the parameters of the Raleigh distributions. $\mathcal{R}_{m,n}(t)$ is the magnitude of the difference $\vec{\mathcal{R}}_m(t) - \vec{\mathcal{R}}_n(t)$, and is Raleigh distributed with parameter $\alpha_{m,n} = \alpha_m + \alpha_n$ and the phase is uniformly distributed over $(0, 2\pi)$.

The X and Y components of the two uniformly distributed Raleigh phasors, $\vec{\mathcal{R}}_m(t)$ and $\vec{\mathcal{R}}_n(t)$, are each approximately Normal with zero mean and variance $= (t/\lambda_m) * (\sigma_m^2 + \mu_m^2)$ and $(t/\lambda_n) * (\sigma_n^2 + \mu_n^2)$ respectively. Since the two nodes move independently according to the random ad-hoc model, the distributions of $X_{m,n}(t) = X_m(t) - X_n(t)$ and $Y_{m,n}(t) = Y_m(t) - Y_n(t)$ are also normal with zero mean and variance $= (t/\lambda_m) * (\sigma_m^2 + \mu_m^2) + (t/\lambda_n) * (\sigma_n^2 + \mu_n^2)$. The result follows by taking the joint distribution of $X_{m,n}(t)$ and $Y_{m,n}(t)$, transforming into polar coordinates and taking the marginal distributions.

Lemma 2.3. The equivalent random mobility vector of node m with respect to node n is the vector difference of the individual random vectors: $\vec{\mathcal{R}}_{m,n}(t) = \vec{\mathcal{R}}_m(t) - \vec{\mathcal{R}}_n(t)$.

Corollary 2.3. By Lemmas 2.2 and 2.3, the equivalent random mobility vector node m with respect to node n is approximately Raleigh distributed and has a uniformly distributed direction.

The results of Subsection 2.2 show that when two nodes move according our random model, the relative movement of one with respect to the other is equivalent to the *difference* between their individual random mobility vectors.

3. Link Availability Model

Link availability provides a statistical prediction of future wireless link status. In this section, the results of the previous section are used to develop models for the distribution of link failure over time for different initial conditions. The section begins with a statement of assumptions and definitions related to link status.

The status of a wireless link depends on numerous system and environmental factors that affect transmitter and receiver range. In general, a node's transmission range is neither fixed, nor symmetric—it demonstrates temporal and spatial variability. In this section, an optimistic approach is adopted for link characterization that is sufficient to meet our modeling objectives. Specifically, it is assumed that the transmission range of a node can be approximated by a circle of fixed radius R_{eq} . If node m is transmitting within such a circle centered at node n , node n is assumed to correctly receive node m 's transmissions. Hence, R_{eq} represents the maximum effective distance at which a given node's transmissions can be received by another node.

Due to unpredictable propagation effects and power variability, unidirectional links are expected to be common in ad-hoc wireless environments. It is shown in Reference [10] that this can have severe effects on ad hoc routing algorithms. Consequently, R_{eq} applies to transmissions in one direction only—in-bound towards the center of the circular transmission region. The following definitions are needed to complete the development of the link availability model:

Definition 3.1. An active link, from node m to node n , is defined as a directed communications link over which node m can transmit data directly to node n without any intermediate nodes. Bidirectional communications require an active link in both directions.

Definition 3.2. $\mathcal{L}_{m,n}(t)$ is an indicator variable which reflects the state of the link directed from node m to node n at time t . $\mathcal{L}_{m,n}(t) = 1$ if the link is active and $\mathcal{L}_{m,n}(t) = 0$ if the link is inactive.

Definition 3.3. Assuming a link directed from node m to node n activates at time $t_0 \geq t$, Link availability is defined as the probability that the link remains active at any time $t \geq t_0$. A link is considered available at time t even if it experienced failure during one or more intervals (t_i, t_j) ; $t_0 < t_i < t_j < t$. More specifically, for nodes m and n , link availability is defined as follows:

$$\mathcal{A}_{m,n}(t) \equiv Pr(\mathcal{L}_{m,n}(t) = 1)$$

3.1. Ad-Hoc Link Availability

The objective is to determine the link availability between a pair of nodes moving according to the random mobility model with known mobility profiles. Corollary 2.3 shows how the joint mobility problem can be transformed into an equivalent problem involving the movement of a single node. In this section, the result of Corollary 2.3, along with the distribution of the distance covered by a single node as it moves across a cell prior to a hand-off [6], is used to derive the distribution of the availability of a link between two nodes.

Figure 2 demonstrates the mobility of two nodes initially separated by a distance D . In Figure 2(a), the two nodes move over an interval of length t : node m moves according to its random mobility vector $\vec{\mathcal{R}}_m(t)$, from position (x_m, y_m) to (x'_m, y'_m) , and node n moves according to $\vec{\mathcal{R}}_n(t)$ from position (x_n, y_n) to (x'_n, y'_n) . The final distance between the two nodes is D' . In Figure 2(b), the position of node n is held fixed while node m is moved according to the equivalent random mobility vector, $\vec{\mathcal{R}}_{m,n}(t)$, from (x_m, y_m) to its new position relative to node n , (x''_m, y''_m) . The transformation from single node random mobility vectors to the equivalent random mobility vector can be seen by noting that $\vec{\mathcal{R}}_{m,n}(t)$ is the vector difference $\vec{\mathcal{R}}_m(t) - \vec{\mathcal{R}}_n(t)$, and by observing how the progression of the distance between the nodes proceeds in an identical manner in Figure 2(a,b). As long as node m lies within the circular region of radius R_{eq} centered at node n , the directed link from node m to node n will be active. The memoryless property of the distribution

of the epoch lengths permits continuous evaluation of the random mobility vectors. Hence, t need not correspond with the end of a mobility epoch.

Depending on the initial status and location of nodes n and m , three cases of link availability are identified. Assuming node n is active at time t_0 , Theorems 3.1, 3.2 and 3.3 characterize the link availability between two mobile nodes, n and m , as reflected by the following initial conditions:

1. Node Activation: Node m becomes active at time t_0 , and is assumed to be at a random location within range of node n .
2. Link Activation: Node m moves within range of node n at time t_0 by reaching the boundary defined by R_{eq} , and is assumed to be located at a random point around the boundary.
3. Initial Distance: Node m is active at time t_0 , and is assumed to be located at a random point a distance of exactly $C \leq R_{eq}$ from node n .

Theorem 3.1 characterizes the the link availability between two mobile nodes m and n at time $t > t_0$. It is assumed that node m becomes active with respect to the ad-hoc network at time t_0 , and is randomly located within transmission range of node n . A complete proof of Theorem 3.1 appears in Reference [4].

Theorem 3.1. Node Activation: *If node n moves according to a random ad-hoc mobility profile, $\langle \lambda_n, \mu_n, \sigma_n^2 \rangle$, and node m activates at time t_0 within a uniform random distance from node n and moves according to a random ad-hoc mobility profile,*

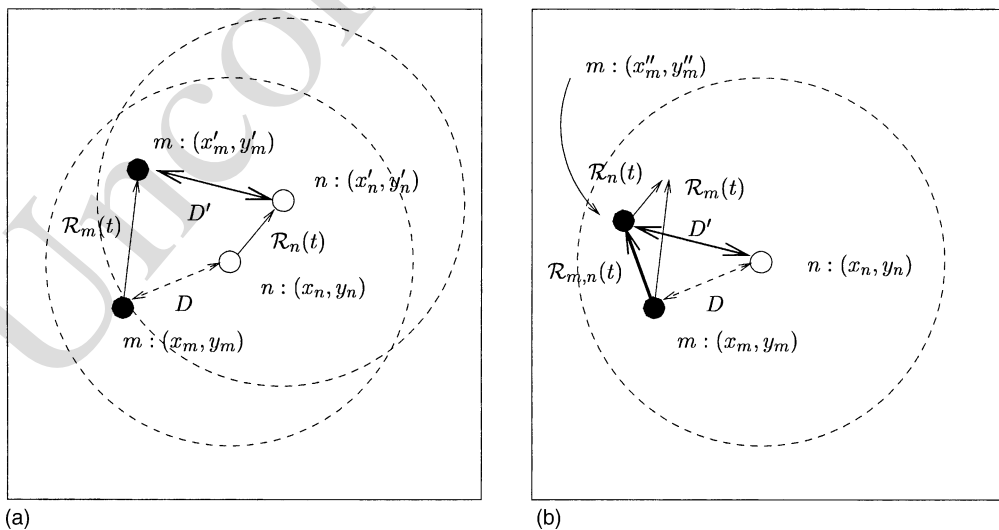


Fig. 2. Joint mobility transformation: (a) joint node case; (b) single node transformation.

$\langle \lambda_m, \mu_m, \sigma_m^2 \rangle$, then the distribution of the link availability over time, $t > t_0$, is given approximately by the following expression, where I_0 and I_1 are hyperbolic Bessel functions, and $\beta = -2R_{eq}^2$:

$$A_{m,n}(t) \approx 1 - \exp\left(\frac{\beta}{\alpha_{m,n}}\right) \left(I_0\left(\frac{\beta}{\alpha_{m,n}}\right) - I_1\left(\frac{\beta}{\alpha_{m,n}}\right) \right)$$

$$\alpha_{m,n} = 2t \left(\frac{\sigma_m^2 + \mu_m^2}{\lambda_m} + \frac{\sigma_n^2 + \mu_n^2}{\lambda_n} \right) \quad (2)$$

Theorem 3.2 characterizes the the link availability between two mobile nodes m and n at time $t \geq t_0$ for the case of Link Activation. It is assumed that a previously inactive link becomes active at time t , with node m randomly located at a distance of R_{eq} from node n . A complete proof of Theorem 3.1 appears in Reference [4].

Theorem 3.2. Link Activation: Let $\langle \lambda_m, \mu_m, \sigma_m^2 \rangle$ and $\langle \lambda_n, \mu_n, \sigma_n^2 \rangle$, be the random mobility profiles of node m and node n respectively, and assume that a link activates between m and n at time t_0 such that m is located at a uniform random point exactly R_{eq} from n , then the link availability is distributed according to the following expression, where I_0 is a hyperbolic Bessel function and $\alpha_{m,n}$ is given by Equation (2):

$$A_{m,n}(t) \approx \frac{1}{2} \left(1 - I_0\left(\frac{-2R_{eq}^2}{\alpha_{m,n}}\right) \exp\left(\frac{-2R_{eq}^2}{\alpha_{m,n}}\right) \right)$$

Theorem 3.3 characterizes the the link availability between two mobile nodes m and n at time $t \geq t_0$ for the Initial Distance case. It is assumed that the distance, C , between m and n is known at time t_0 .

Theorem 3.3. Initial Distance: Let $\langle \lambda_m, \mu_m, \sigma_m^2 \rangle$ and $\langle \lambda_n, \mu_n, \sigma_n^2 \rangle$, be the random mobility profiles of node m and node n respectively, and assume that a link is active between them at time t_0 , such that m is located at a uniform random point at a distance $C \leq R_{eq}$ from n , then the link availability is distributed according to the Rice–Nakagimi distribution [5] expressed below, where $\alpha_{m,n}$ is given by Equation (2):

$$A_{m,n}(t) = 1 - \int_{R_{eq}}^{\infty} \frac{2r}{\alpha_{m,n}} \exp\left(\frac{-(r^2 + C^2)}{\alpha_{m,n}}\right) I_0\left(\frac{-2rC}{\alpha_{m,n}}\right) dr$$

Proof

Lemma 3.1. Let the distance between two mobile nodes, m and n , at time t be given by $\mathcal{D}_{m,n}(t)$. The link

availability can be expressed with respect to this distance as follows:

$$A_{m,n}(t) \equiv Pr(\mathcal{D}_{m,n}(t_0 + t) \leq R_{eq} | \mathcal{D}_{m,n}(t_0) \leq R_{eq}).$$

Lemma 3.1 relates the distance between two nodes at time t to the link availability. The result of Theorem 3.3 is derived by recognizing that $\mathcal{D}_{m,n}(t)$ can be expressed as the sum of the equivalent random mobility vector $\vec{\mathcal{R}}_{m,n}(t)$ and a constant length vector \vec{C} . The relationships among these variables are depicted in Figure 3. The result of Theorem 3.3 is exactly the solution of the general problem of finding the sum of a uniformly distributed Raleigh vector and a constant. The complete derivation can be found in Reference [5]. The idea is to decompose $\vec{\mathcal{R}}_{m,n}(t)$ into its normally distributed X and Y components, and to add C to the X component by observing that the axis can be aligned with C due to the uniform assumption with respect to the initial position of node m . The components remain normally distributed; however, the X component now has mean $= C$. For $d \geq 0$, $0 \leq \theta \leq 2\pi$, the joint distribution of $\mathcal{D}_{m,n}(t)$ and θ_D is given by the following expression:

$$f_{\mathcal{D}_{m,n}(t), \theta_D}(d, \theta) = \frac{d}{\pi \alpha_{m,n}} \exp\left(\frac{-(d^2 + C^2)}{\alpha_{m,n}} + \frac{2dC \cos \theta}{\alpha_{m,n}}\right).$$

To obtain the desired distribution, take the marginal distribution with respect to $\mathcal{D}_{m,n}(t)$, by integrating

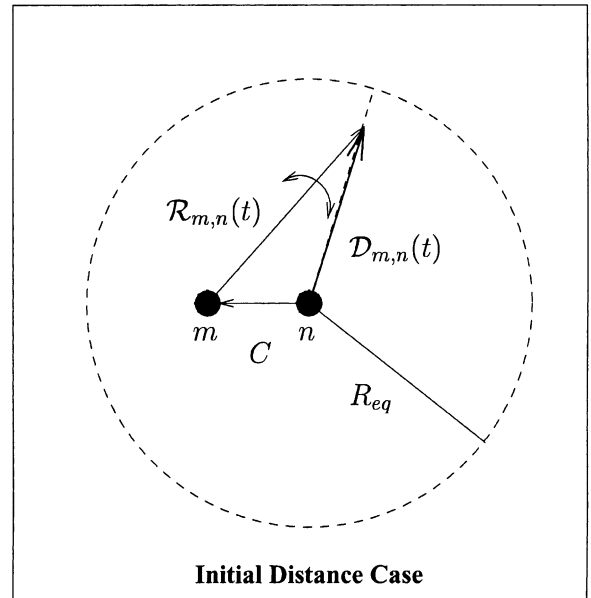


Fig. 3. Ad-hoc link availability models: initial distance.

Equation (3.1) over $(0, 2\pi)$ and using the following integral expression for the modified Bessel function of order zero [5]. The result follows immediately:

$$f_{\mathcal{D}_{m,n}(t)}(d) = \frac{2d}{\alpha_{m,n}} \exp\left(\frac{-(d^2 + C^2)}{\alpha_{m,n}}\right) I_0\left(\frac{2dC}{\alpha_{m,n}}\right)$$

QED

3.2. Series Link Availability

This section presents analysis of the joint probability distribution of series link availability given independent node mobility. The analysis in Reference [11] demonstrated that the probability of survival of any two links sharing a node are dependent. The concept of ‘fate-sharing’ can be extended on a hop-by-hop basis, wherein, the survival of each subsequent link is constrained by conditions that enabled the previous link in the path to survive. For the present analysis, the following definition is given to extend the concept of link availability over an entire path and Lemma 3.2 completes the model developed in this chapter by relating path availability to the individual link availabilities.

Definition 3.4. Let $\mathcal{P}_{i,j}^k(t)$ be an indicator variable that reflects the status of path k from node i to node j at time t . $\mathcal{P}_{i,j}^k(t) = 1$ if all the links in the path are active at time t , and $\mathcal{P}_{i,j}^k(t) = 0$ if one or more links in the path are inactive at time t . The availability of path k , $\Pi_{i,j}^k(t)$, between nodes, i and j , at time $t \geq t_0$ is given by the following probability expression:

$$\prod_{i,j}^k(t) \equiv Pr(\mathcal{P}_{i,j}^k(t) = 1)$$

Based on this definition, the question arises as to how the individual link availabilities should be used to characterize path availability. In ABR, the individual link associativities are assumed to be additive, but paths can only be compared if they have the same hop-count. Short paths with larger aggregate associativity are preferred. However, the aggregate metric should ideally reflect the contribution of the *weakest* link. ABR assumes that all links that have survived beyond the associativity threshold are stable. Hence, path selection is insensitive to weak links.

In general, the calculation of the path availability is a difficult problem because it depends on knowledge of the correlation among the the individual link availabilities. Consequently, in practice it may be useful to select paths that maximize their minimum availability (bottleneck) link. Such an approach may be useful in comparing paths of the same length similar to ABR. However, without knowledge of how link failures are correlated, it becomes difficult to extend this approach for comparing paths of different lengths.

Based upon the stated assumption of independent link failures, the following lemma expresses a well-defined path availability metric:

Lemma 3.2. Let $A_{m,n}(t)$ be the availability of link (m, n) along path k between nodes i and j at time t as defined in Definition 3.3. According to the assumption of independent link failures, the availability of path k at time t , $\Pi_{i,j}^k(t)$, is given by:

$$\prod_{i,j}^k(t) \equiv Pr(\mathcal{P}_{i,j}^k(t) = 1) = \prod_{(m,n) \in k} A_{m,n}(t) \quad (3)$$

Despite independent mobility, the assumption of independent link failures is only an approximation that provides a lower bound on path availability. To understand why this is the case, consider two links that share a common node. Specifically, consider a sequence of nodes along path: m, n, p with two links: $\mathcal{L}_{m,n}$ and $\mathcal{L}_{n,p}$. The path availability is simply the joint probability of these two links being active at some time t : $Pr(\mathcal{L}_{m,n}(t) = 1, \mathcal{L}_{n,p}(t) = 1)$. Using conditional probability, this is equivalent to the following: $Pr(\mathcal{L}_{n,p}(t) = 1 | \mathcal{L}_{m,n}(t) = 1)Pr(\mathcal{L}_{m,n}(t) = 1)$. Clearly, if the link availabilities are independent this yields the result of Lemma 3.2. However, both sides of the conditional probability $Pr(\mathcal{L}_{n,p}(t) = 1 | \mathcal{L}_{m,n}(t) = 1)$ involve node n . By conditioning on the status of the link from n to m , the position of node n is being *constrained*. Thus, precise evaluation of the conditional probability would reflect a smaller state space of possible positions for node n .

Reducing the state space increases the probability of survival of the second link. Hence, the actual path availability is greater than the product of the individual availabilities. Consider the problem of determining the joint availability of two series links: (m, n) and (n, p) —the two links are subject to fate sharing because they share a common node, n . Based on previous definitions and results, the joint availability

Q7

for a two link path can be stated as follows, wherein, the random variables Z_m and Z_p represent the distribution of the distance a node must travel (from its initial position/condition) before reaching the transmission threshold [3,6] and the final expression results from a standard transformation:

$$\begin{aligned}
Pr(\mathcal{L}_{n,m}(t) = 1, \mathcal{L}_{n,p}(t) = 1) &= Pr(\mathcal{L}_{n,p}(t) = 1 | \mathcal{L}_{n,m}(t) = 1) Pr(\mathcal{L}_{n,m}(t) = 1) \\
&= Pr(R_{n,p}(t) \leq Z_p | R_{n,m}(t) \leq Z_m) \mathcal{A}_{m,n}(t) \\
&= Pr(R_n(t) - R_p(t) \leq Z_p | R_n(t) - R_m(t) \leq Z_m) \mathcal{A}_{m,n}(t) \\
&= Pr(R_n(t) \leq R_p(t) + Z_p | R_n(t) \leq R_m(t) + Z_m) \mathcal{A}_{m,n}(t) \\
&= \frac{Pr(R_n(t) \leq Z_p + R_p(t), R_n(t) \leq Z_m + R_m(t))}{Pr(R_n(t) \leq Z_m + R_m(t))} \mathcal{A}_{m,n}(t) \\
&= Pr(R_n(t) \leq Z_p + R_p(t), R_n(t) \leq Z_m + R_m(t)) \\
&= Pr(R_n(t) \leq \min(Z_p + R_p(t), Z_m + R_m(t))) \\
&= \int_0^\infty Pr(R_n(t) \leq g) f_{G=\min(Z_p+R_p(t), Z_m+R_m(t))}(g) dg \tag{4}
\end{aligned}$$

Equation (4) is the general solution for the two-hop problem. However, no general closed-form solution has been found to this problem. Hence, the product-form solution obtained using the independent link failure assumption is sufficient to meet the objectives of this research.

Lemma 3.2 provides a metric which represents a probabilistic measure of path availability. This metric can be used by the routing algorithm to favor more stable paths, or to select paths which support a lower bound, α , on availability over an interval of length t as specified in the following expression:

$$\prod_{i,j}^k(t) \geq \alpha \tag{5}$$

A path meeting these criteria is referred to as an (α, t) -path. (α, t) -path routing could be used to ensure that all paths meet a minimum stability requirement. Based on Lemma 3.2 and Equation (5), the availabilities of each of the links along a path are used to determine if the path is an (α, t) -path. The extension to include the effects if random node fails in our model can be made by considering the link failure probabilities conditioned on the status of the nodes. The total probability of link failure consists of the weighted contribution due to mobility and to the failure of at least one of the nodes. In the following section, simulation is used to validate the link availability model for the node and link activation initial conditions. Experiments demonstrate, as expected, that the model remains a valid model for arbitrary distributions of node velocity—including models that include random length pauses or sleeping modes.

4. Model Validation

In this section, the analytical model for link availability is validated. This is achieved through comparison of link availability as evaluated using the analytical expressions to observed values as estimated

using discrete event simulation. The question that must be answered is how well do the predicted values match observed results when the assumptions underlying the model hold? To answer this question, a pair of nodes were simulated moving according to the random-independent model with a variety of mobility profiles and speed distributions. The simulation was used to estimate link availability between the nodes at discrete instances over a range of time. Simulation data were collected to reflect both of the initial conditions—node and link activation.

Based on the assumptions used in the derivation of the analytical expressions, it is known that precision depends on satisfaction of the CLT with respect to the distributions of the mobility vectors. The criteria for satisfying the CLT require the number of independent mobility epochs to be sufficient large during the observation interval. Hence, better agreement is expected between the simulation and the analytical models as the the product λt increases. Larger values of λ imply a greater number of mobility epochs during a fixed interval of time, and larger intervals of time imply a greater number of mobility epochs given a fixed mean epoch length. Both of these conditions increase the number of independent random variables whose summation is approximated by a Normal distribution in the derivation of Lemma 2.1. Moreover, it is expected that precision will improve with increasing transmission range. The reason for this is that link survival is directly proportional to transmission range. Hence, increasing the transmission range will also increase the number of mobility epochs observed over a fixed interval of time for any value of λ ; mobility

epochs cannot contribute to the accuracy of the model after the link has failed.

The simulation results demonstrate very good agreement with the analytical model for large values of λt . In each case, the two models converge rapidly with increasing time. As expected, the model also performs better as transmission range is increased. For epoch lengths of 30 s, the link activation model was extremely accurate at predicting the actual probabilities—for small values of t , the model was within 2% in the *worst* case given a fixed transmission range of 250 m. The worst case reflected the highest mean velocity. The node activation model was somewhat less accurate for the smallest values of t . However, for a fixed transmission range of 250 m, it was generally within 10%. The small t error increases with increasing epoch length, as expected, since the CLT may not be satisfied; however, results were still acceptable for all values of t for 60 s epoch lengths. A description of the simulation model is presented in Section 4.1, followed in Section 4.2, by analysis of the simulation data and comparison to the analytical results.

4.1. Simulation Model

A simulation model was developed consisting of two processes representing the nodes at each end of a wireless link. The startup conditions for Theorem 3.1 specify that the two nodes are initially located randomly within range of one another, whereas the initial conditions for Theorem 3.2 require one node to be randomly located at a distance of R_{eq} from the other. Each simulated node moved according to its own random mobility profile which was specified as input to the simulation.

During each simulation run, the nodes moved over a range of observation times. Specifically, each experiment consisted of 40 evenly spaced 3 min intervals from $t = 0$ to 120 min. At the start of each run, the initial position of the nodes was randomly determined according to the requirements of the model as stated previously. The position of each node was then determined at the end of each interval and used to calculate the distance between them. The link status was then determined based upon the transmission distance threshold.

Automatic run-length control was built into the simulation model to achieve a desired level of accuracy in estimating the probabilities. Specifically, the model was designed to stop after finding the probability of link availability for *every* observation point with 95% confidence intervals (CI) at a relative precision of 0.05.

The simulation language *CSIM* [12] provides functionality to compute confidence intervals using the method of batch means [13]. For each observation time, the proportion of runs for which the link was found to be active was used as an estimate of link availability. The following list specifies a set of experiments that were conducted:

1. The first set of experiments were designed to evaluate the *node activation case* assuming the speed of each node was *Normally distributed*.[†] The mean epoch length was fixed at 30 s and the mean speed was varied from 2.5 to 25.0 kph with a standard deviation (SD) of 2.0. Each experiment was repeated for four transmission ranges between 100 and 1000 m.[‡]
2. The second set of experiments were designed to evaluate the *link activation case* given the assumption that the speed of each node was *Normally distributed*. The mean epoch length was fixed at 30 s and the mean speed was varied from 2.5 to 25.0 kph with a SD of 2.0. Each experiment was repeated for four transmission ranges between 100 and 1000 m.
3. The third set of experiments repeated the first two experiment sets using *Uniformly distributed speed*. The max and min values of the Uniform distribution were chosen to achieve the same mean and standard deviation as used for the Normally distributed speed experiments.
4. The fourth set of experiments repeat the first two experiment sets using modified distributions for speed by including a 50% *probability of remaining stationary* ($v = 0$) during any mobility epoch. The mean and standard deviation of the speed were chosen to achieve the same aggregate mean and standard deviation as used for the Normally distributed speed experiments. Hence, when moving the mean speed ranged from 5.0 to 50.0 kph.
5. The final set of experiments repeated the first two experiment sets except that the mobility epoch length was varied—data were collected for epoch lengths from 60 to 240 s.

In the remainder of this section, we discuss the simulation results and compare them to the predicted probabilities of the analytical model.

[†]Negative speed from the Normal distribution corresponds to positive speed in opposite direction.

[‡]Transmission ranges were selected to represent a fair range of currently available commercial outdoor point-to-point radio systems.

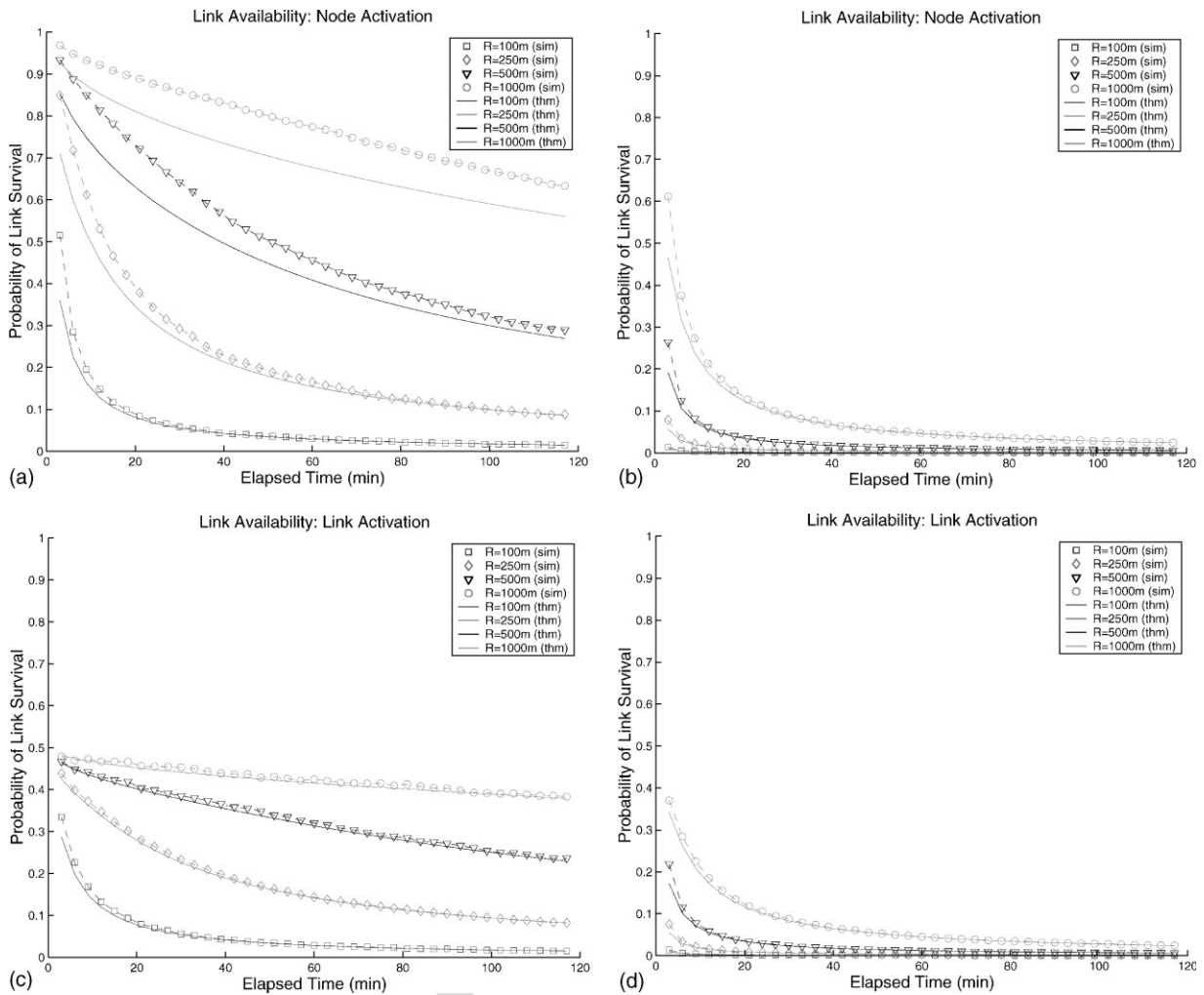


Fig. 4. Comparison of simulation results to analytical model: (a) $N(\mu = 2.5 \text{ kph}, \sigma = 2.0), 1/\lambda = 30 \text{ s}$; (b) $N(\mu = 25.0 \text{ kph}, \sigma = 2.0), 1/\lambda = 30 \text{ s}$; (c) $N(\mu = 2.5 \text{ kph}, \sigma = 2.0), 1/\lambda = 30 \text{ s}$; (d) $N(\mu = 25.0 \text{ kph}, \sigma = 2.0), 1/\lambda = 30 \text{ s}$.

An overall analysis of the simulation results is presented in this subsection. Several representative examples from Experiment Set-1 through Set-4 are plotted in Figure 4(a–d) and Figure 6(a–d) and discussed in this subsection. Each figure represents a specific mobility profile and compares the simulation results to the analytical results for each of the four values of transmission range, R_{eq} . In the figures, the solid curves represent the analytical results and the dashed curves show the 40 points of evenly spaced simulation data. Each simulation point represents the probability of link survival at a 95% confidence level—each analytical point was evaluated directly from the expressions in Theorems 3.1 and 3.2. A complete set of plots for all the data from the simulation experiments can be found in Reference [4].

4.2. Output Analysis

Figure 4(a) and (b) plot the results of the node activation model from Experiment Set-1 for $\mu = 2.5$ and $\mu = 25.0$ kph respectively. The figures show link availability versus elapsed time. As the mean speed is increased, link availability decreases dramatically for each value of R_{eq} . This result is consistent and corresponds to intuitive expectations. Visual inspection of the figures suggests that the analytical model provides a lower-bound on the observed link availability that is generally within 10% and much tighter in most instances. The results for smaller values of t improve with larger transmission range and slower mean speed, and the simulated data tend to converge toward the model with increasing t .

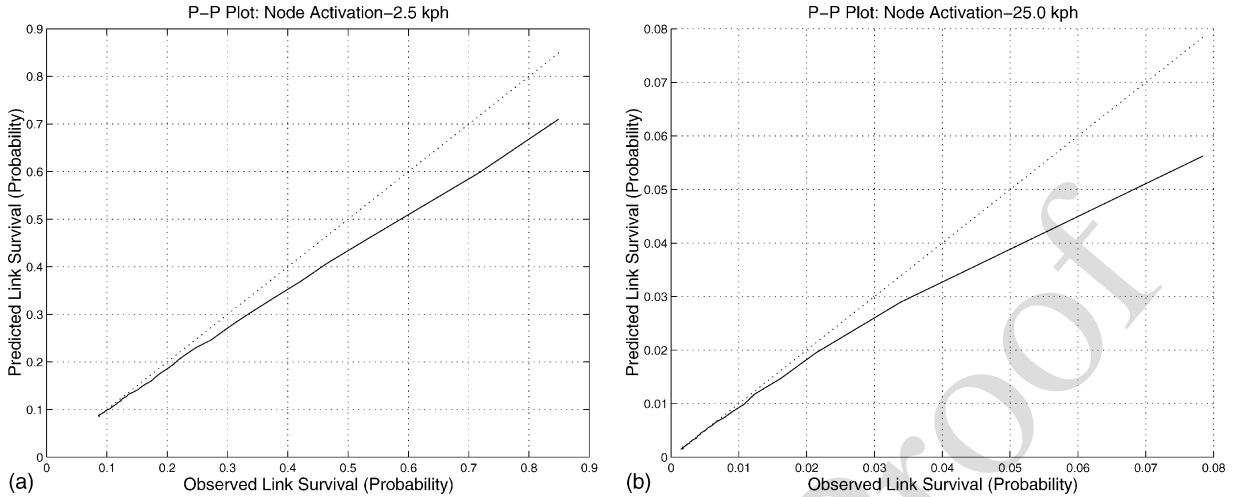


Fig. 5. P-P plots for node activation data: (a) velocity: $N(\mu = 2.5 \text{ kph}, \sigma = 2.0)$; (b) velocity: $N(\mu = 25 \text{ kph}, \sigma = 2.0)$.

The P-P plots in Figure 5(a) and (b) correspond to data from the same set of experiments for $R_{eq} = 250 \text{ m}$. These plots demonstrate the properties of the model more clearly. The solid curves show the deviation of the model from the observed values (note the scales for the two figures). The higher probabilities correspond to smaller values of t . That is, the region where link survival is *more* likely. Although the relative error is larger in the 25.0kph case, it represents an underestimate of roughly 2.0%. Whereas, the maximum error in the 2.5 kph, case is approximately 15.0%.

Although in the time domain, the node activation model appears to provide reasonable results, the P-P plots reveal why a χ^2 statistical goodness-of-fit test may result in rejection of the null hypothesis (H_0). Namely, using the equiprobable approach in implementing a χ^2 test results in more heavily weighting the contribution due to small values of t in the time domain. That is, the statistical test that can produce the most valid results will emphasize the regions where the model performs at its worst. Hence, the χ^2 test is not going to show how well the model converges, nor is it going to validate how good the lower bound provided by the model may be.

Table I. χ^2 goodness-of-fit test for node activation data.

Mean velocity	χ^2 -Test statistic		
	Normal	Uniform	Normal with pause
2.5	1.50	13.75	11.45
5.0	18.7	14.58	10.52
10.0	10.3	27.38	5.61
20.0	15.45	20.41	26.21
25.0	25.81	45.21	20.70

Despite the potential shortcomings of goodness-of-fit testing for evaluating this type of model, a sample of numerical results are presented in Table I. Specifically, using the equiprobable approach a χ^2 test was performed on the node activation model for Normal, Uniform and Normal with pause models with $R_{eq} = 1000 \text{ m}$. The sample size for each test, $n = 100$, was chosen to be relatively small since the χ^2 test tends to almost always reject the null hypothesis, H_0 , when the sample size is large [13] due to the fact that it picks up small differences between the distributions. For each test, the distribution was divided into ten equiprobable intervals. Since the parameters of the fitted distribution are known, the comparison statistic is χ^2 with 9 df. For $\alpha = 0.05$, the value of $\chi^2(0.05, 9) = 15.507$. Hence, in the case of Normally distributed speed, we cannot reject H_0 for any case except for the highest speed. For the Uniform case, H_0 must be rejected at $\alpha = 0.05$ for 10.0 kph through 25.0 kph; and for the random pause case, H_0 must be rejected in the 20.0 and 25.0 kph cases. Observe that the χ^2 test emphasizes the inability of the model to be precise for small values of t . Hence, the apparent disagreement for higher speed movement, which results in the highest density of link failures close to $t = 0$. However, despite this shortcoming, the model provides a lower bound that is tight and has the potential to improve path selection relative to non-predictive metrics.[§]

[§]The majority of ad-hoc routing algorithms adopt a pseudo-random approach to path selection without direct regard to path survival. Current exceptions include ABR, SSA and (α, t) -Cluster.

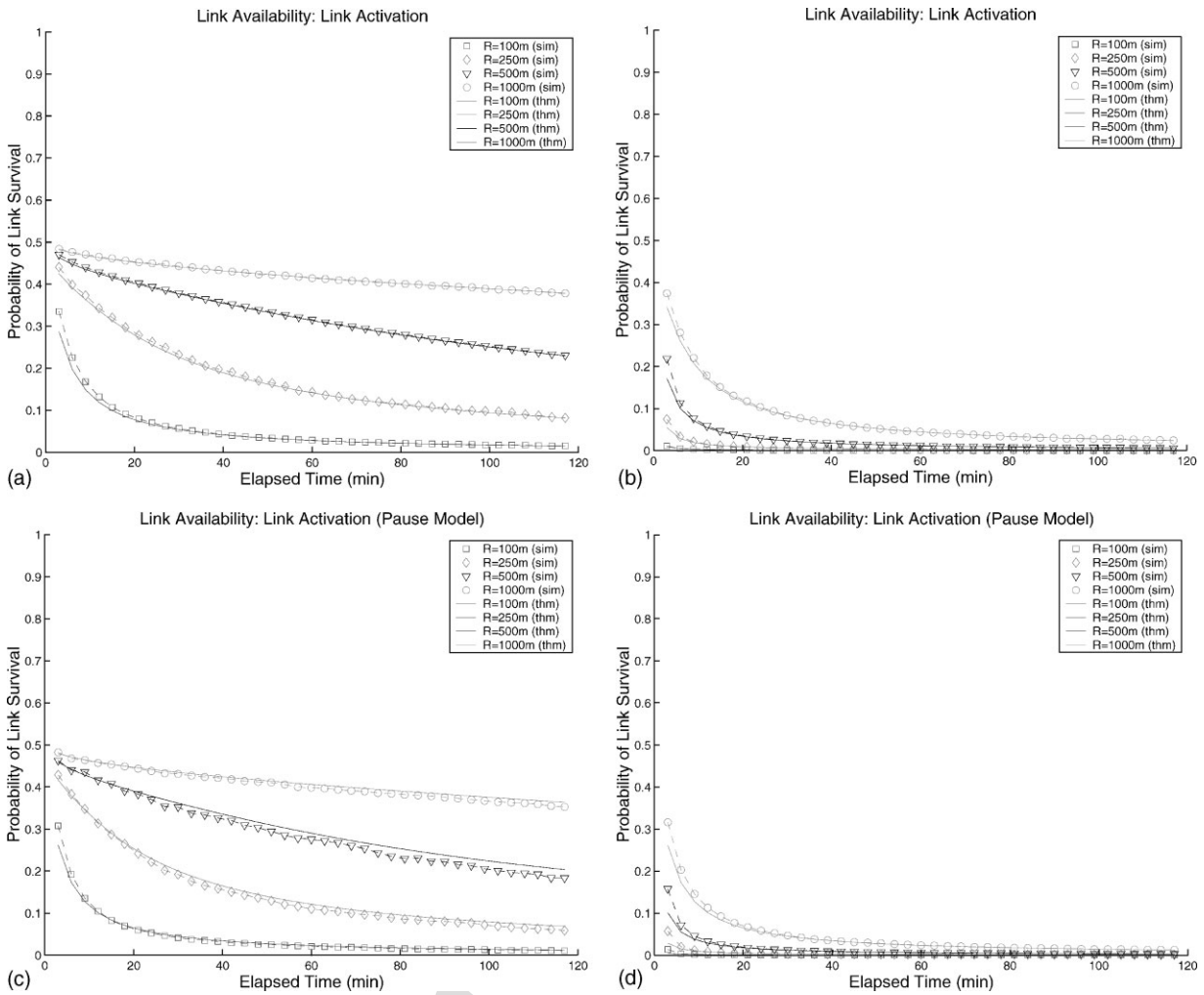


Fig. 6. Comparison of simulation results to analytical model: (a) $U(\mu = 2.5 \text{ kph}, \sigma = 2.0)$, $1/\lambda = 30 \text{ s}$; (b) $U(\mu = 25.0 \text{ kph}, \sigma = 2.0)$, $1/\lambda = 30 \text{ s}$; (c) $N(\mu = 5.0 \text{ kph}, \sigma = 2.0)$, $1/\lambda = 30 \text{ s}$; (d) $N(\mu = 50.0 \text{ kph}, \sigma = 2.0)$, $1/\lambda = 30 \text{ s}$.

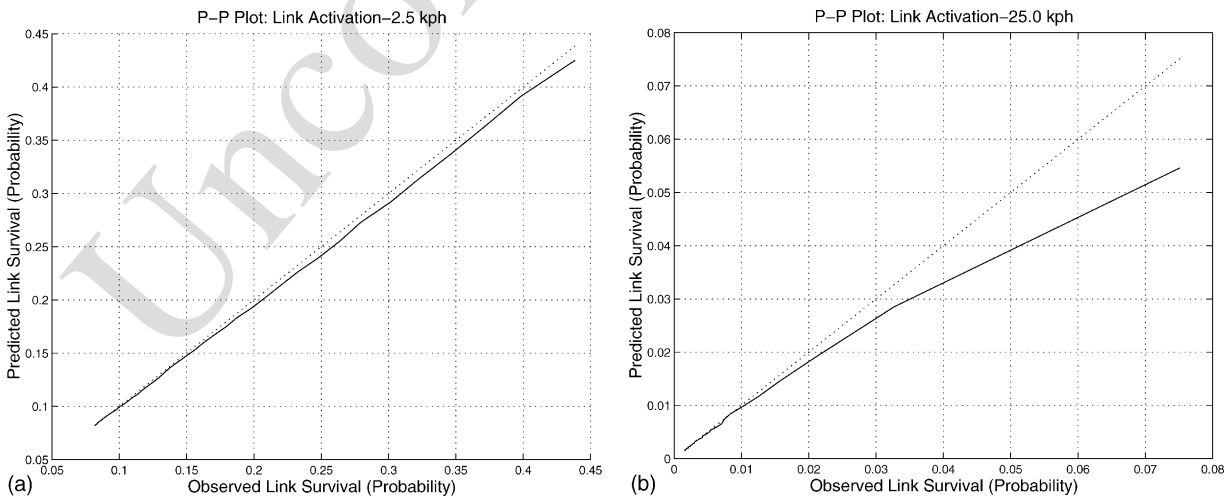


Fig. 7. P-P plots for link activation data: (a) velocity: $N(\mu = 2.5 \text{ kph}, \sigma = 2.0)$; (b) velocity: $N(\mu = 5.0 \text{ kph}, \sigma = 2.0)$.

Table II. χ^2 goodness-of-fit test for link activation data.

Mean velocity	χ^2 -Test statistic		
	Normal	Uniform	Normal pause
2.5	8.27	9.54	16.77
5.0	10.84	7.52	4.46
10.0	9.92	6.81	8.81
20.0	15.32	6.79	6.75
25.0	23.82	10.45	11.45

Figure 4(c) and (d) plot the results of the link activation model from Experiment Set-1 for $\mu = 2.5$ and $\mu 25.0$ kph respectively. The plots validate the assertion that there is a 50% probability of immediate link failure due to the initial node positions. They also suggest close agreement between the observed data and the model in nearly every instant. Visual inspection does show that for very small values of t there is a difference between the curves. These differences are most apparent for smaller values of R_{eq} and for higher mean velocity. However, the P-P plots in Figure 7(a) and (b) show that although the differences may be statistically significant, their effect is not likely to be substantial. The data used for the P-P plots correspond with Experiment Set-2 at $R_{eq} = 250$ m. The fit at 2.5 kph has a maximum difference of approximately 1%, whereas the maximum difference at 25.0 kph approaches 2%.

The same set of χ^2 tests were repeated for the link activation case; however, the initial link availability at time $t = 0^+ = 0.50$ so 5 equiprobable intervals of $P = 0.10$ were used. Thus, there were only 4 df. The data are shown in Table II based on the P-P plots, we expected the results of the χ^2 test on the link activation data to be superior to the node activation data. However, the test still places the greatest emphasis on the small t regions. Hence, out of 15 tests, a total of 5 lead to rejection of H_0 in both cases. For $\alpha = 0.05$, the value of $\chi^2(0.05, 4) = 9.488$. Hence, H_0 must be rejected in the Normally distributed speed case for $\mu = 10.0$ through $\mu = 25.0$ kph. However, for the Uniform and the pause models, H_0 must be rejected at $\alpha = 0.05$ only for $\mu = 25.0$ kph.

Figure 6(a) and (b) show results for the link activation case from Experiment Set-3 in which speed was Uniformly distributed. The figure show examples for 2.5 and 25.0 kph. Visual inspection suggest that the match between the simulated data and the model is very good. This is verified by the results of the χ^2 test as shown in in Table II. Finally, data from Experiment Set-4 are plotted in Figure 6(c) and (d). These data

reflect results for the link activation case in which there was a 50% probability that each node remains stationary during any given mobility epoch. The speed during epochs in which a node moved was Normally distributed with μ ranging from 5.0 to 50.0 kph in order to achieve the same aggregate mean speeds as in the previous experiments.

As expected for large enough values of λt , the results corresponding to the same cases were relatively insensitive to the distribution of the speed given the same aggregate mean and standard deviation. Hence, the same model is able to capture the desired probabilities regardless of whether speed is Normally distributed, Uniformly distributed or if it includes random length pause times. The only requirement is that the aggregate mean and standard deviation of the speed should be known. We are not able to claim that the results for the different distributions are strictly statistically identical due to the differences that are apparent for small values of t . This discrepancy is expected since the CLT is not applicable in those regions.

Considering the conditions required for CLT to hold, the simulation results provide persuasive evidence for the validity of the expressions for link availability derived in Section 3.1. [The system parameters used in the simulations cover, the full range of expected operational values for transmission range^{Q8}](#), node speed and epoch duration. For large values of R_{eq} , the model holds reasonably well even for small t . For smaller values of R_{eq} , the model converges very rapidly to the simulation results.

The remaining data pertaining to the Experiment Sets 1–4 were consistent with the preceding discussion. Data for these experiments appear in References [4,14]. The data from Experiment Set-5 examined the effects of increasing the mean epoch length on the accuracy of results. Data were collected assuming Normally distributed speeds for epoch lengths ranging from 60 to 240 s. As expected, the model becomes less precise with increasing epoch length. This result is especially significant for small values of t and large values or mean velocity. However, even where the model fails to be precise, it still consistently provides a lower bound in all the cases we tested.

5. Routing Performance

The results presented in the previous section showed with high statistical confidence that the analytical models for link availability are very accurate except in regimes where CLT does not hold. Thus, they

provide an excellent measurement of the long-term characteristics of links between randomly moving node pairs. However, an important question remains unanswered. Random-independent mobility provides a good first-order engineering approximation, however, it does not fully characterize the range of mobility scenarios possible. Hence, what is the practical impact of this metric on routing performance, and what else can be learned from these results?

In this section, the performance of the mobility-based routing metric is measured under a realistic model for node movement in a large ad-hoc network. Specifically, the case is considered in which nodes move according to multiple-group dynamics. As such, correlated movement is assumed among nodes within a given group, and the past movement of a given node is assumed to affect its future movement. To capture these effects in a discrete-event simulation, the Hierarchical-Group-Mobility (HGM) Model proposed in Reference [15] was utilized. The experiments consisted of measuring the path survival times computed according to different metrics over a range of mobility levels. The results show that the link-availability metric significantly outperforms both shortest-path and fixed-threshold based routing schemes [1] except at the extremes—for example, under *very high mobility* in which less than 10% of the *optimal or longest possible surviving* paths lasted more than 70s. Also, in the lowest mobility scenario, there was very little difference among the metrics which all approach optimal survival.

5.1. Mobility Modes and Group Mobility

Two fundamental models can be defined for the mode of interaction among nodes in an ad hoc network,

namely, *task-oriented* and *service-oriented*. Task oriented networks consist of users working towards a common goal; whereas, in a service-oriented network there are no such relationships. Based on the mode, both mobility and communications patterns may vary considerably. In a hybrid network, all modes coexist in time and space. HGM captures group dynamics and independent movement over all small, medium and large geographical areas. Thus, HGM captures characteristics of more realistic node mobility and can be used to model a wide range of mobility scenarios. In HGM, *mobility* is not measured simply by mean node velocity. The mobility level (0.0–1.0) is reflective of the degree of intra-group versus inter-group movement, and the frequency with which nodes remain stationary or move over various distances. Speed is assumed to be correlated to the distance of a *move*. Hence, mobility reflects the level of correlation, speed and distance covered by the nodes.

Figure 8 depicts how two common measures of mobility relate as metrics to the mobility level as used in HGM. Figure 8(a) shows the non-linear relationship between mean node velocity and the mobility level as defined by HGM. At the lowest levels of mobility, nodes move slowly and are tightly associated with a single group. As mobility increases, more nodes start to move from group to group at a higher velocity and over greater ranges than most intra-group movement. Thus, mean velocity increase rapidly at first. However, the rate of increase begins to decline once the probability of changing groups exceeds 50%. Observe also that velocity is insensitive to the size of the network. Figure 8(b) shows a metric that has been suggested as a better measure of mobility than velocity. The

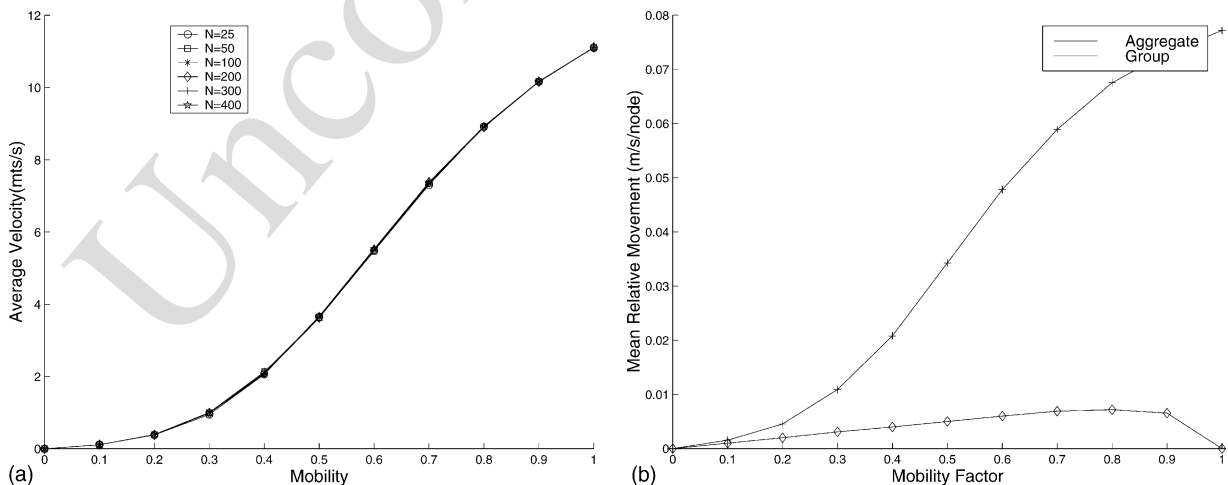


Fig. 8. Mobility metrics: (a) mean velocity versus mobility; (b) mean relative movement versus mobility.

mean-relative-movement is a measure of the relative association among the nodes. How rapidly are they moving away from each other? Values ranged from 0 to 0.08 m/s. In the figure, the value has been normalized and is depicted for both the aggregate, and for intra-group movement. As expected, nodes within a group generally stay relatively close to each other. The drop to zero at the highest mobility level is due to the artifact that no node remains in a group at the highest mobility level in HGM. These figures depict a model that captures the complexity of group dynamics, thus meeting our objectives.

5.2. Simulation Model and Results

For the simulation, a 200 node network was modeled. Transmission range was assumed to be 200 m and mobility was based on the HGM model with an average group size of 6 nodes and velocity ranging from 0 to 11 m/s (40 kph). In HGM, velocity depends on the mobility *state* of the node. A node may be *at rest*, *moving within a group*, *moving between nearby groups* or *moving between groups over large distances*. The resulting rate of link status change ranged from 0–50 per second. Routes were computed *off-line* between all pairs of nodes according to three metrics: (1) Shortest-Path (SP) (hop-count); (2) Fixed-Threshold Stability Scheme; and (3) Link-Availability using the product form for the path value. For the Fixed-Threshold, the threshold yielding the optimal result was used in each case. The paths were observed over an interval of 120 s to determine the probability of path survival at each instant with a 95% confidence level and precision of 0.05. If any link along the

selected path failed, the path was considered to have failed. At the conclusion of the 120 s interval, using only links that were active over the entire interval of time, the probability of finding a path between all pairs of nodes was determined. This value represented the *optimal-path* or longest surviving path.

Low mobility is characterized by a high probability that nodes remain associated with a given *group* over time. Furthermore, low mobility implies sporadic movement of relatively short distances and low velocity interspersed with *at-rest* periods. Figure 9(a) presents comparison of the probability of path survival for each of the three routing metrics against the optimal path over a 120 s interval for *Mobility* = 0.10. The rate of link status change was 0.01 link up/down per-node per-second ($\Delta/n/s$), the aggregate relative movement was 0.002 m/s and the mean velocity was 0.2 m/s. The routing performance was somewhat surprising as very little difference was expected. However, the mobility-based metric performed significantly better than alternative approaches. Results showed a 15% improvement relative to SP and 7.5% relative to optimal fixed threshold routing. At *Mobility* = 0.30, each of the mobility metrics increased by a factor of five ($5 \times$). As expected, the differences in routing performance also increased. Figure 9(b) shows that the new metric achieves a 50% improvement in survival times over SP routing and a 40% improvement relative to optimal fixed threshold routing.

Increasing mobility into the moderately-high range further improves the performance of the mobility-based metric, however, the differences among the metrics begin to taper off rapidly in time. At

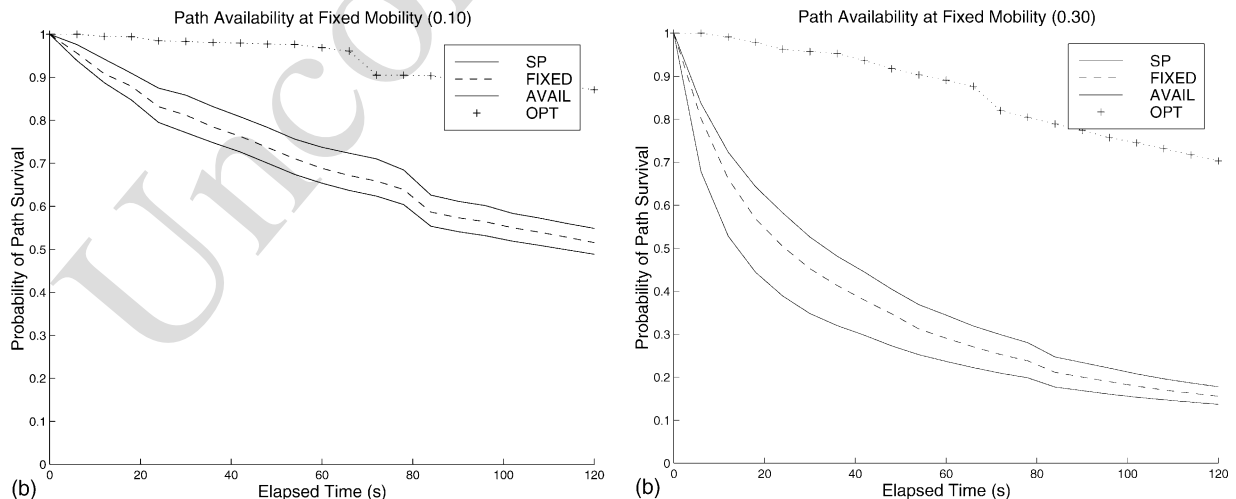


Fig. 9. Path survival versus elapsed time by routing metric: (a) mobility level = 0.10; (b) mobility level = 0.30.

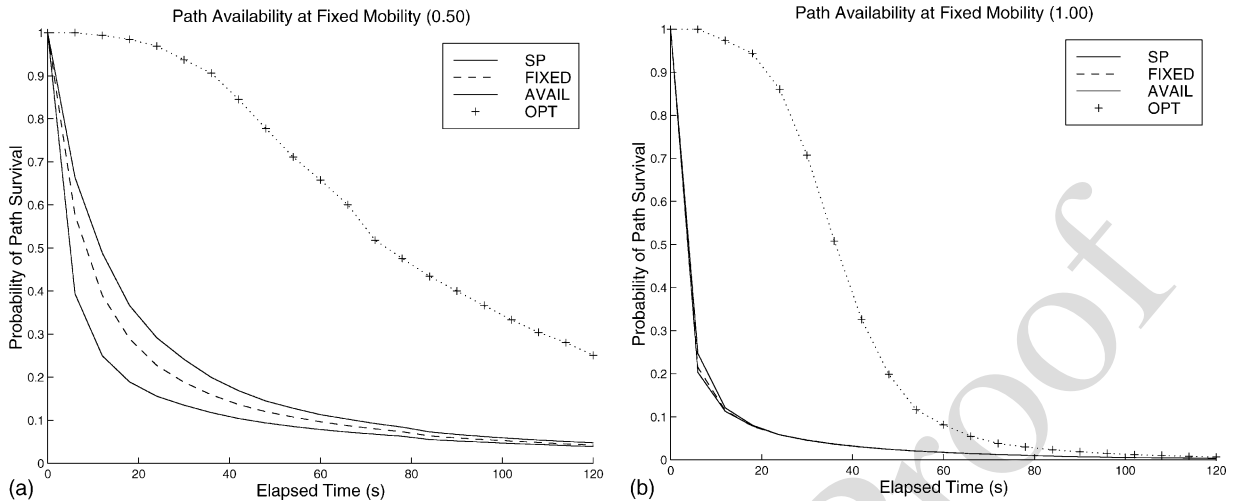


Fig. 10. Path survival versus elapsed time by routing metric: (a) mobility level = 0.50; (b) mobility level = 1.00.

Mobility = 0.50 depicted in Figure 10(a), link status changed at a rate of $0.2 \Delta/n/s$, relative movement increased to 0.035 m/s and mean velocity rose to 4.0 m/s. The link-availability routing metric improves survival times by 100% over SP routing and 50% over fixed-threshold routing; however, the differences remain significant for approximately 60 s. By 80 s, there is very little difference between the metrics. Improved path survivability in the range of 60 s can lead to significantly reduced routing overhead. Furthermore, it enables improved support for quality-of-service (QoS) routing by leveraging the time to re-route delay or throughput sensitive traffic. At a high mobility level of 0.70 with a mean velocity of 8.0 m/s, very brief improvement was observed. Specifically, up to approximately 20 s the new metric achieves a 50% improvement over the other approaches. However, they rapidly converge after 30 s.

The final plot, which is shown in Figure 10(b), illustrates the highest level of mobility—the rate of link status change exceeded $0.5 \Delta/n/s$, aggregate relative movement was 0.08 m/s and the mean velocity was 11.0 m/s. In HGM, this level of mobility represents the *most* chaotic state. Nodes move rapidly over large distances and never associate themselves with a group. This type of movement is effectively *random-independent* mobility. Thus, as quantified here, random-independent mobility is *pessimistic* with respect to routing, contradicting claims that it represents an *optimistic* assumption. At maximum mobility, there are no differences among the routing metrics. Furthermore, observe that *less than* 10% of the optimal paths survive longer than 60 s. This result suggests a *very important* observation, namely,

optimal prediction is insufficient to ensure path quality in large networks; hence scalable solutions to routing in ad hoc networks must combine predictive mechanisms with other strategies, for example, adaptive clustering, multiple-level dynamic hierarchies and dispersity based multi-path routing. This assertion is based on the observation that in a moderate sized network of 200 nodes, the lower bound on the probability of any path failing within 60 s is 90%. Thus, an algorithm capable of finding optimal routes must engage in path repair for 90% of all active communications once a minute. Under these conditions, stability would become difficult to maintain. Depending on traffic conditions and the efficiency of the re-routing algorithms persistent backlogs would begin to grow and eventually choke off the dissemination of routing information and lead to the congestion collapse of the network.

6. Conclusions

Mobility is a crucial element affecting the control and organization of ad-hoc networks. This article represents a first-order approximation for statistical estimation of link availability based on analytical modeling of random mobility. It is the first such model developed for ad-hoc networks. The main results validate the analytical model and demonstrate that it outperforms existing routing strategies in terms of path survival under group-based mobility scenarios in a moderate sized network.

In this article, the problem of predicting the probability of link survival over time was examined. The results build and improve upon our related work in

References [3,15–17]. Unlike our previous work, this article presents a thorough validation of the derived analytical results using simulation and statistical analysis. Moreover, a routing performance study was included to demonstrate the usefulness of the mobility-based routing metric subject to *realistic* mobility scenarios. Other attempts to factor node mobility into the routing process have adopted a methodology based upon predefined timing thresholds that are intended to identify stable links [1,2].

Our analytical framework adopts a link status model identical to those used in References [6,7,11,18] based upon the *transmission circle* model. A more detailed propagation model is proposed in Reference [19], however, it requires terrain information and does not incorporate an analytical mobility model. The transmission circle model assumes that omni-directional antennas are utilized. The emergence of *smart antenna* arrays [20], that are able to adapt the shape of their transmission region to their environment, support the feasibility of such a model. Simulation analysis shows that our model provides an analytically valid solution to the link availability problem based on the stated assumptions which depend on three mobility parameters referred to as the mobility profile of the node. This consists of the mean and standard deviation of node speed and the mean epoch duration. The only requirement for implementation is that nodes have access to approximate localization information in order to determine their mobility parameters [11,19,21–23].

We present a closed-form solution to the link availability problem based upon a reasonable set of first-order assumptions. Using link availability as a routing metric simulation results demonstrate substantial improvement in route longevity relative to both shortest-path and fixed-threshold based stability schemes subject to group mobility dynamics and a range of mobility intensities; thus validating our main hypotheses. However, no scheme was able to approach optimal longevity beyond minimal mobility levels. We believe that abstract models are limited in this realm, thus, real-time measurement based trajectory prediction methodologies are needed. Finally, our results demonstrate that in large dynamic networks path longevity is very short, hence, optimal prediction is insufficient to ensure path quality. Continuous path reconstruction is not feasible. We, therefore, assert that predictive mechanisms alone are insufficient to ensure scalable routing solutions. The idea of scalability can either be abandoned as an intractable problem in dynamic environments, or, alternatively,

attention can be focused on multi-mode routing strategies that utilize implicit or explicit hierarchies to separate the routing task into multiple domains.

References

- Toh C-K. Associativity-based routing for ad-hoc networks. *Wireless Personal Communications* 1997; **4**(2).
- Dube R, et al. Signal stability based adaptive routing (SSA) for ad-hoc networks. *IEEE Personal Communications* 1997.
- McDonald AB, Znati T. A mobility based framework for adaptive clustering in wireless ad-hoc networks. *IEEE Journal on Selected Areas in Communications (J-Sac), Special Issue on Ad-Hoc Networks* 1999; **17**(8).
- Bruce McDonald A. A mobility-based framework for adaptive dynamic cluster-based hybrid routing in wireless ad hoc networks. PhD thesis, University of Pittsburgh, Pittsburgh, PA, 2000.
- Beckmann P. *Probability in Communication Engineering*. Harcourt, Brace & World, Inc.: New York, 1967.
- Hong D, Rappaport S. Traffic models and performance analysis for cellular mobile radio telephone systems with prioritized and nonprioritized handoff procedures. *IEEE Transactions on Vehicular Technology* 1984; **35**(3).
- Guerin R. Channel occupancy time distribution in a cellular radio system. *IEEE Transactions on Vehicular Technology* 1987; **35**(3).
- Benveniste M. Probability models of microcell coverage. *Wireless Networks* 1996; **2**(4).
- Zonoozi M, Dassanayake P. User mobility modeling and characterization of mobility patterns. *IEEE Journal on Selected Areas in Communications* 1997; **15**(7).
- Prakash R. Unidirectional links prove costly in wireless ad-hoc networks. In *Proceedings of DIMACS Workshop on Mobile Networks and Computers* 1999.
- Basagni S, Chlamtac I, Faragó A, Syrotiuk VR, Talebi R. Route selection in mobile multimedia ad hoc networks. In *Proceedings of the Sixth IEEE International Workshop on Mobile Multimedia Communications, MOMUC'99*, San Diego, CA, 15–17 November 1999.
- Schwetman H. *CSIM Users Guide*. Microelectronics and Computer Technology Corp., 1992.
- Law A, Kelton WD. *Simulation Modeling and Analysis*. McGraw-Hill, 1991.
- Bruce McDonald A. NEU web site. <http://www.ece.neu.edu/faculty/mcdonald/downloads>, 2001.
- Rao S, McDonald AB, Znati T. Design and analysis of hierarchical group-based mobility for ad-hoc wireless network. In *Proceedings of WCN-CNDS Modeling and Simulation Conference*, Phoenix, AZ, January 2001 (to Appear in).
- McDonald AB, Znati T. A path availability model for wireless ad-hoc networks. In *Proceedings of the IEEE Wireless Communications and Networking Conference 1999 (WCNC'99)*, New Orleans, LA, September 1999.
- McDonald AB, Znati T. Predicting node proximity in ad-hoc networks: a least overhead adaptive model for electing stable routes. In *Proceedings of the First IEEE/ACM Workshop for Mobile Ad Hoc Networking and Computing (MobiHOC)*, August 2000.
- Sanchez M, Manzoni P, Haas Z. Determination of critical transmission range in ad-hoc networks. Draft of article: <http://www.ee.cornell.edu/misan/paper-web.ps>, 1999.
- Broch J, Punnoose R, Nikitin P, Stancil D. Optimizing wireless network protocols using real-time predictive propagation modeling. In *Proceedings of the IEEE Radio and Wireless Conference 1999*, Denver, CO, August 1999.

20. Thompson JS, Grant PM, Mulgrew B. Smart antenna arrays for CDMA systems. *IEEE Personal Communications* 1996; 3(5).^{Q2}
21. Park VD, Corson MS. A highly adaptive distributed routing algorithm for mobile wireless networks. *IEEE Infocom 1997*.^{Q3}
22. Ko YB, Vaidya NH. Location-aided routing (LAR) in mobile ad-hoc networks. In *Proceeding of ACM/IEEE MOBICOM*, October 1998.
23. Basagni S, Chlamtac I, Syrotiuk VR. Dynamic source routing for ad hoc networks using the global positioning system. In *Proceedings of the IEEE Wireless Communications and Networking Conference 1999 (WCNC'99)*, New Orleans, LA, 21–24 September 1999.

Q6 Authors' Biographies

A. Bruce McDonald earned Ph.D. and M.S. degree from the University of Pittsburgh (2000, 1995) and a B.S. degree in Electrical Engineering from Northwestern University (1986). He is currently Zraket assistant professor of Electrical and Computer Engineering at Northeastern University in Boston. Prof. McDonald's research interests include routing algorithms, communications protocols, ad hoc networks, wireless communications, and simulation and performance evaluation. His current focus is on cross-layer interaction, optimization and QoS support for real-time applications in dynamic wireless networks. He has served as the Program Chair for the SCS Communications Networks and Distributed Systems Conference (CNDS'02 and

CNDS'03) and has served on several other Conference Program Committees. From 1996 to 2000, he served as a senior computer engineer in the Department of Neurophysiology at Children's Hospital of Pittsburgh and in 1996, he was a visiting researcher in the Applied Network Research Group at Bellcore in Redbank NJ.

Taieb F. Znati obtained a Ph.D. in Computer Science at Michigan State University, East Lansing, in April 1988, and a Master of Science Degree at Purdue University, West Lafayette, Indiana. In 1988, he joined the University of Pittsburgh where he currently serves as a professor in the Department of Computer Science with a joint appointment in the Department of Information Science and Telecommunications. Prof. Znati's research interests focus on agent-based technology, middleware, the design of network protocols for wired and wireless communication networks to support multimedia applications' QoS requirements, the design and analysis of medium access control protocols to support distributed real-time systems, network simulation, and the investigation of fundamental design issues related to large scale distributed systems. He is frequently invited to present lectures and tutorials and participate in panels related to networking and distributed multimedia topics, in the United States and abroad. He is currently on leave from the University of Pittsburgh to serve as senior program director for Networking Research at the National Science Foundation.

Q6

Author Query Form (WCM/135)

Special Instructions: Author please write responses to queries directly on Galley proofs and then fax back. Alternatively please list responses in an e-mail.

Q1: Author: Please provide 3–5 Keywords.

Q2: Author: Please provide page range

Q3: Author: Please provide vol no. and page range

Q4: Author: Please provide publisher's location.

Q5: Author: Please update

Q6: Author: Please provide photo of Authors

Q7: Author: Please check, OK?

Q8: Author: Please check the sentence.

Uncorrected Proof